




Article

Characterization of Ingested Plastic Microparticles Extracted from Sea Turtle Post-Hatchlings at Necropsy

Keon Beigzadeh ¹, Julie M. Rieland ² , Catherine B. Eastman ³, David J. Duffy ^{3,4}  and Brian J. Love ^{1,2,5,*} 

¹ Department of Materials Science and Engineering, University of Michigan, 2300 Hayward St., Ann Arbor, MI 48109, USA; keonbe@umich.edu

² Program in Macromolecular Science and Engineering, University of Michigan, 2300 Hayward St., Ann Arbor, MI 48109, USA; jmriel@umich.edu

³ Whitney Laboratory for Marine Bioscience and Sea Turtle Hospital, University of Florida, St. Augustine, FL 32080, USA; cbeastman@whitney.ufl.edu (C.B.E.); duffy@whitney.ufl.edu (D.J.D.)

⁴ Department of Biology, University of Florida, Gainesville, FL 32611, USA

⁵ Biomedical Engineering, University of Michigan, 2300 Hayward St., Ann Arbor, MI 48109, USA

* Correspondence: bjlove@umich.edu

Abstract: Inadvertent consumption of latent microplastics is a lethal challenge for developing creatures in aquatic environments. There are compelling needs to classify which kinds of plastics are most likely to be encountered by sea creatures and to develop mitigation strategies to reduce exposure. We analyzed an ensemble of microplastic particle fragments isolated from sea turtle post-hatchlings to identify their composition and other features and attributes. These microplastic particles were likely consumed by post-hatchlings because of the adsorbed biofilm formation mimicking normal food sources. Of the hundreds of particles that were collected, 30 were selected for analysis using differential scanning calorimetry (DSC), Fourier transform infrared (FTIR) spectroscopy and density assessment to identify them compared with other compositional libraries. These thermophysical measurements were also compared with observational assessments via optical microscopy. Of the particles tested, nearly all were polyolefins such as polyethylene and polypropylene. The melting points of the extracted polymers were typically lower than for product grades of these resins, indicative of some level of degradation. Spectral analysis by FTIR often showed absorption indicative of new chemistries likely from both hydrolysis and biofilm growth observed on the surface that was subsequently investigated through surface abrading. Separate assessments of density of these particles were conducted and tended to reinforce identification via FTIR and DSC. The density results can be misleading if additives, fillers or biofilms that form alter the particle density relative to those of the neat resins. We suggest that since post-hatchlings commonly feed in the neritic or nearshore environment, less dense polymers are more likely to convey, thereby threatening sea turtle hatchlings who consume them inadvertently.

Keywords: sea turtle; microplastic; characterization; biofilms



Citation: Beigzadeh, K.; Rieland, J.M.; Eastman, C.B.; Duffy, D.J.; Love, B.J. Characterization of Ingested Plastic Microparticles Extracted from Sea Turtle Post-Hatchlings at Necropsy. *Microplastics* **2022**, *1*, 254–262.

<https://doi.org/10.3390/microplastics1020018>

Academic Editor: Nicolas Kalogerakis

Received: 9 March 2022

Accepted: 8 April 2022

Published: 13 April 2022

Publisher's Note: MDPI stays neutral with regard to jurisdictional claims in published maps and institutional affiliations.



Copyright: © 2022 by the authors. Licensee MDPI, Basel, Switzerland. This article is an open access article distributed under the terms and conditions of the Creative Commons Attribution (CC BY) license (<https://creativecommons.org/licenses/by/4.0/>).

1. Introduction

Latent plastics discarded into rivers, streams, lakes and oceans are not just eyesores but can have profound physical and health impacts on reptiles and animals that coexist in these aquatic ecosystems. There is growing concern towards macroplastics, which can degrade and fractionate into smaller pieces through exposure to ultraviolet light, reactive enzymes and general aging, which can result in particles that when eaten can obstruct digestive organs of aquatic species, resulting in their general decline in nutritional health. It is also possible that microplastics already present in the environment can be conveyed into estuaries and streams through stormwater runoff as already formed microplastic particles [1–5]. Microplastics, if consumed and conveyed through the ecosystem from smaller organisms up the food chain (i.e., biomagnification), can encounter humans in commercially acquired

fish having consumed these plastic-filled organisms as feed fish [3,6–8]. These concerns have been increased by the discovery of microplastics found in fish moving through the commercial food market [5,7].

Closer to shore, microplastics are found in sediments conveyed through surf zone interactions derived from the aquatic environment and runoff from terrestrial sources [2,9–12]. Several demographic assessments of collected microplastics from mammals, shellfish and other aquatic species have been performed, comparing the particles from colorimetric, size, shape, texture and compositional perspectives [1,7,13–15]. With polymers having much lower densities than metals and ceramics, which are more likely to immediately sink, aquatic microplastic exposure is more likely to be depth-dependent and polymer-dependent. Lower density polyolefins such as polyethylene and polypropylene have more comparable densities to water and are more likely to be buoyant and suspended in aqueous reservoirs.

Aquatic vertebrate mortality is particularly important with endangered species, such as several types of sea turtles found in Northeast Florida. Every sea turtle post-hatchling that succumbs from ingesting microplastics is a casualty to subsequent breeding efforts and thwarts other efforts to boost turtle prevalence to reduce their threat assessment as endangered species [1,14,15]. Hence, we analyzed microplastic samples among groups of particles that had been extracted from these endangered sea turtles [13] to assess what they are likely consuming and identify other sample features that may support efforts to address the microplastic exposure problem.

2. Materials and Methods

2.1. Field Samples

Samples of microplastics were received for analysis from the Sea Turtle Hospital at the University of Florida Whitney Laboratory for Marine Bioscience. These specimens were extracted from turtle post-hatchling gastrointestinal tracts during necropsies performed in 2016 [13]. These post-hatchlings were stranded (washed ashore) in Northeast Florida. Post-necropsy, samples were processed as described elsewhere [13]. Briefly, the specimens were washed in a 10% H₂O₂ solution to remove any residual organic matter, using methods adapted from sediment particle size distribution analysis [16]. Inorganic material was then rinsed a minimum of three times with deionized water and specimens were then filtered and evacuated to remove moisture before storage. Thirty of the larger and flatter samples were selected and sent to the University of Michigan to characterize their structure primarily by calorimetry and spectroscopy. Plastic specimens were received as treated, and we did not observe the surfaces before the peroxide exposure. The only constraint on the particle selection was that they were ideally flat and large enough for appropriate spectral analysis. Samples were also used as prepared for pycnometry and optical microscopy. Thus, very small microplastic samples were not amenable for analysis using all techniques.

2.2. Fourier Transform Infrared Spectroscopy in Reflectance Mode (FTIR)

Microplastics were first characterized by attenuated total reflectance Fourier transform infrared spectroscopy (FTIR-ATR) (Jasco FT/IR 4100, Jasco, Inc, Easton, MD, USA) using a 1.0 cm⁻¹ resolution within the frequency range of 4000–600 cm⁻¹. FTIR is non-destructive and allowed further characterization by calorimetry and pycnometry.

Of the collected samples, flat specimens with areas ranging between 1 and 4 mm² were selected for analysis using FTIR reflectance measurements. Non-destructive FTIR spectral measurements were taken initially on the as-received surfaces and again after some modest sectioning to assess the composition of the bulk polymer below any adsorbed biofilm. Particles were abraded by clamping the particle between tweezers and shaving the surface with a straight blade. Samples were clamped to the surface of the ATR reflection crystal before analysis. The clamp force was sufficient in some instances to fracture the more brittle samples, but even post-fracture their composition was still analyzable. Survey

spectra were plotted after performing a 25-point adjacent average smoothing routine and annotating the peaks using OriginPro 2020b (Northampton, MA, USA).

2.3. Differential Scanning Calorimetry (DSC)

Since more common microplastics such as polyethylene (PE) and polypropylene (PP) are semicrystalline, assessments of any potential melting transitions of these samples were tracked using a Perkin Elmer Pyris 6 (Perkin Elmer Corporation, Waltham, MA, USA) differential scanning calorimetry (DSC). Sample masses ranging from 3–8 mg were placed into aluminum sample pans and were heated from room temperature to 300 °C, then cooled to room temperature with a heating/cooling rate of 20 °C/min under a nitrogen inert gas purge with a volumetric flow rate of 20–40 cm³/min. Raw data for the heat flow as a function of both temperature and time allowed for determination of melting and crystallization temperatures, as well as the corresponding temperatures of these transitions. Post-processing and analysis was performed with the TA Instruments TRIOS package (TA Instruments, New Castle, DE, USA).

2.4. Density Measurements: General Methodology

Density values were assessed using a fluid density assessment protocol adapted from Gal et al. [17]. Selected plastic samples were placed in deionized water to assess their overall buoyancy relative to water (0.997 g mL⁻¹). Those with a density less than water were assessed using a sink–float titration assay. Here, 3–4 samples were measured at a time. Particles and flakes were immersed in pure methanol (0.792 g mL⁻¹) in a graduated cylinder, which sunk due to their comparatively higher density relative to the solvent. Deionized water was added in 0.75 mL increments until a particle rose to a suspended state in solution, indicating the fluid had attained an equivalent density to the suspended particle (Figure 1). In the case of over-shooting the density—marked by the particle floating at or just below the meniscus—adding more methanol can return the particle to the bottom of the vessel (Figure 1).

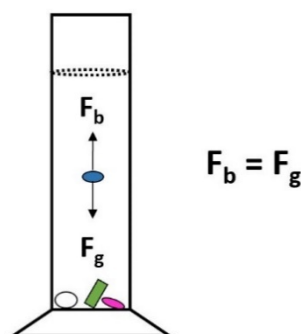


Figure 1. Schematic of fluid density assessment by submersion in methanol–water solution.

The density of the solvent at the sink–float transition was collected and measured using a pycnometer (Thermo Fisher, Waltham, MA, USA). Solvent density values were determined using Equation (1), where M_{pl} is the mass of the pycnometer containing the equivalent-density liquid. M_{pa} is the mass of the pycnometer containing air (empty). V_p is the volume of the pycnometer and ρ_a is the density of air at room temperature (0.00192 g mL⁻¹ at 23 °C). For specimens denser than water (0.997 g mL⁻¹), the density was measured directly using the pycnometer when sufficiently large particles (>~2 mm³) were available. For direct measurement of particles, Equation (2) was used, where M_{ps} is the mass of the pycnometer and sample, M_p is the mass of the empty pycnometer, M_{pw} is the

mass of the pycnometer filled with deionized water, M_{pws} is the mass of the pycnometer filled with the sample and deionized water and $\rho_w = 0.997 \text{ g mL}^{-1}$ at 23°C .

$$\rho_l = \frac{M_{pl} - M_{pa}}{V_p} + \rho_a \quad (1)$$

$$\rho_s = \frac{(M_{ps} - M_p) * \rho_w}{(M_{pw} - M_p) - (M_{pws} - M_{ps})} \quad (2)$$

3. Results

To ensure that the 30 samples assessed in this paper were representative of the larger sample sets observed from previous necropsies, the selected samples were assessed using the typical qualitative assessments applied in the literature [1,10,11,13–15,18,19] (Figure 2). The form factor distribution of the 30 plastic pieces sub-sampled for characterization resembled the larger dataset from the >2000 specimens collected from all post-hatchlings [13].

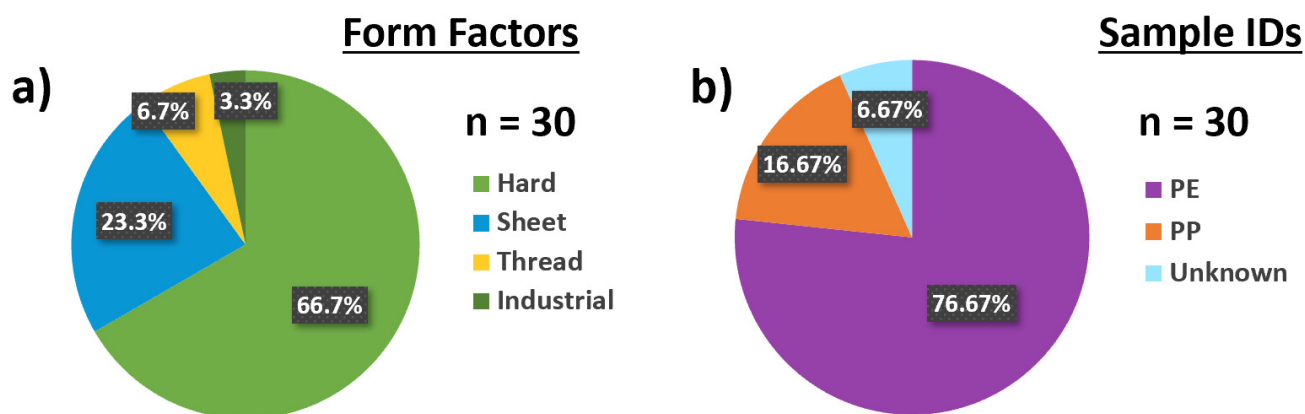


Figure 2. Distributions of sample identities and form factors: (a) form factor distribution of the 30 plastic pieces sub-sampled for characterization as part of this study [13]; (b) sample type distribution (PE, PP or unknown) of the plastic pieces evaluated.

The samples that were large enough were first analyzed by non-destructive FTIR followed by thermal characterization in the DSC (Supplementary Table S1). Separate sample fragments were used for pycnometry.

The DSC and pycnometry measurements were representative of the bulk of each fragment. Figure 3 shows example DSC thermogram plots during the heating for microplastic PE and PP samples. Both fragments showed lower than expected melting temperatures. Typical melting points for as-made PE and PP were ~ 140 and 165°C , respectively. Both microplastic thermograms featured an extended tail in their melting endotherms indicative of smaller chain lengths [20]. These examples in Figure 3 were broadly representative of the sample set (Supplementary Table S1).

The pycnometry results ranged from 0.88 to 1.008 g mL^{-1} (Supplementary Table S1) and are shown in the box and whisker plots in Figure 4, fractionated by those most likely to be PE and those most likely to PP, representing 28 of the 30 measured samples. The resolved average densities were 0.970 g mL^{-1} for PE and 0.943 g mL^{-1} for PP and the ranges encapsulated by the upper and lower quartiles of each were 0.955 – 0.984 and 0.918 – 0.970 g mL^{-1} , respectively. The densities for both sets were higher than anticipated, particularly for PP, with an expected density range in the order of 0.895 – 0.92 g mL^{-1} [21]. One plausible rationale is that suppliers often add fillers such as calcium carbonate, chalk or some other valueless mass to decrease the material cost by improving the efficiency of the resin usage.

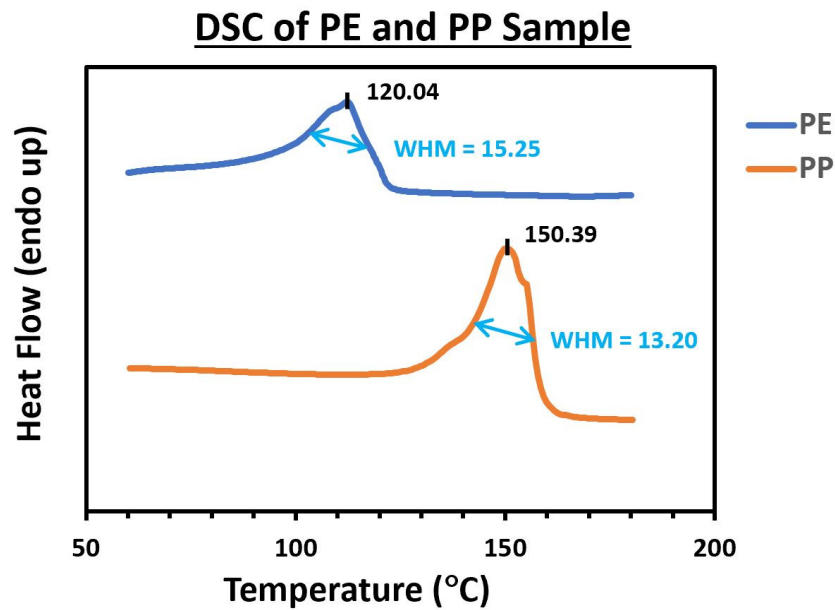


Figure 3. Example DSC endotherms of samples identified as PE and PP. The peak melting temperature for hatchling-extracted PE sample melts at ~120.0 °C. The PP sample melts at 150.4 °C. WHM indicates the melting peak width at half-max. In both cases, the endotherm contours for both samples are rather broad, with an extended low melting point tail.

Density Distributions

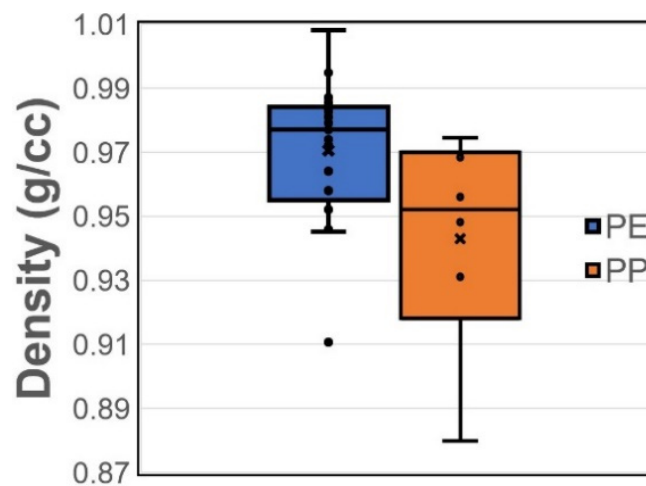


Figure 4. Density distributions of samples identified as PE and PP.

The ATR-FTIR reflection measurements and absorbances indicative of the outermost 1 μm depth of the microplastic surface were also performed. The spectra also show other spectral absorbances not commonly found in virgin resins masking the polymer absorption, making polymer identification more challenging. Figure 5 shows a sample with observed surface biofilm interference (Figure 5a) having been physically abraded down to the bulk of the polymer (5b) and reanalyzed by FTIR. Analysis of the scraped surface yielded a much cleaner spectrum, confirming the bulk polymer structure. After abrasion, the microplastic spectrum clearly matched up with the spectrum of bulk PE [22].

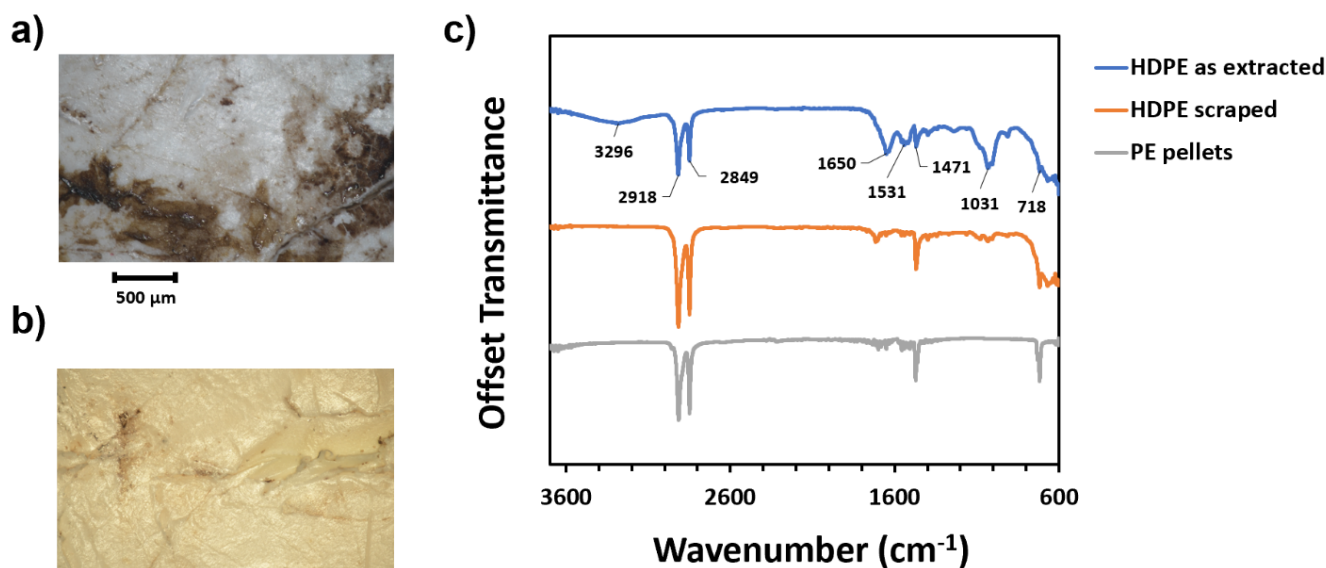


Figure 5. PE sheet sample reanalyzed with FTIR after having biofilm residue scraped from the surface. This sample was identified as HDPE based on density assessments: (a) micrograph of surface as extracted; (b) micrograph of surface after scraping biofilm (~1 mm below the surface) with a razor; (c) corresponding FTIR spectra of the as-extracted and scraped samples compared alongside standard PE pellets.

Markers of degradation might manifest themselves as strong carbonyl absorption usually in the range of $1600\text{--}1800\text{ cm}^{-1}$. We noted some absorption in this range as well, but could not definitively confirm polymer deterioration, as proteins in biofilms might also show similar vibrational absorption. It is noted that most of the absorption in the 1600 range was absent following scraping, suggesting that most of this absorption was likely from biofilms.

4. Discussion

Addressing the form factor assessment, the distribution of microplastic form factors agreed with the original much larger sample size of over 2000 plastic particles from which the plastic specimens were selected [13]. The 30 sample forms we analyzed were representative of the larger-scale data set from the ecosystem of the Northeast Florida coast [13].

Nearly all samples extracted from the post-hatchlings (28 of 30 evaluated) were either PE or PP, lighter density polymers that are more likely to float near the ocean surface or at least in the neritic zone when consumed. High-buoyancy (low-density) litter is more affected by Stokes drift toward shores and beaches. Our results support the assertion that hatchlings are more vulnerable to this lower density plastic. In fact, the density values of all but one of the samples were below 1.025 g mL^{-1} , the average density of ocean water [23], suggesting that these particles likely exist at or near the ocean surface or in the near-shore environment, where they are ultimately consumed. It is possible that microplastic particles of other compositions exist and if they settle and are found on the sea floor, they will be consumed by other species. Particles of higher density, such as nylon or polyester, would settle quicker and be more likely to be found settled into deeper waters and not observed as prevalently in the surf zone.

Surface skimming polymers are more prone to biofilm growth, since algae exist in the upper 60–90 m of ocean water [24] and are also susceptible to higher UV exposure [9,25]. Chain fracture events induced by UV could explain the observed peak broadening and lower melting points of the extracted polymers that were evaluated. Our work corroborates

the work by Longo et al., who reported lower melting points, often by as much as 10 °C lower than the bulk polymers following UV exposure [26].

Lastly, the individual characterization measurements were tedious and required larger samples for IR, DSC and density analysis. Many microplastic specimens, defined as 1 µm to 5 mm [3], might not be large enough to use the tools applied here. The presented techniques are most applicable with larger microplastics, but addressing the throughput remains a hurdle for more efficient particle identification. Trends in current research suggest a strong interest in developing faster and more efficient analysis techniques for handling larger sets of microplastic samples [27–29], although the resolution for assessing small and impure samples remains a difficulty. However, if there were ways to characterize smaller samples or do real-time imaging, such as with Raman imaging, higher throughput might be achievable. The same artifacts of biofilm formation we encountered might still require countermeasures for accurate identification.

5. Conclusions

Thirty microplastic specimens collected from turtle post-hatchlings at necropsy were analyzed using a range of techniques. Most of the samples analyzed were composed of polypropylene (17%) and polyethylene (77%). Their low densities facilitate their conveyance in the nearshore environment. There were some noted reductions in the melting points of these fragments, confirming other research findings and consistent with some degree of breakdown due to environmental exposure. There was also some biofilm growth noted via FTIR, suggesting why post-hatchlings might mistake these microplastic particles for food. The biofilms do not penetrate throughout the bulk of the particles and can be mechanically abraded away, leading to more accurate polymer composition identification. This observational study specifically considered the materials consumed by post-hatchlings. Reducing the load of microplastic waste in general and making microplastic surfaces less receptive to fragmentation and biofilm formation can help reduce the risk of lethal consumption of these fragments by vulnerable post-hatchlings and other aquatic life.

Supplementary Materials: The following supporting information can be downloaded at: <https://www.mdpi.com/article/10.3390/microplastics1020018/s1>, Table S1: Summary of key sample characterization data, including the compositional identity, form factor, density and peak melting temperature.

Author Contributions: Conceptualization: K.B., C.B.E., D.J.D. and B.J.L.; methodology, K.B., C.B.E., D.J.D. and B.J.L.; formal analysis: K.B.; resources: C.B.E., D.J.D. and B.J.L.; data curation: K.B., J.M.R. and B.J.L.; writing: all.; review and editing: all.; supervision; B.J.L. and D.J.D.; project administration: B.J.L. and D.J.D.; funding acquisition: D.J.D. All authors have read and agreed to the published version of the manuscript.

Funding: This research was generously funded by The Sea Turtle Conservancy, Florida Sea Turtle Grants Program under grant number 21-004R, and the National Save The Sea Turtle Foundation, Inc. (Ft. Lauderdale, USA) under grant number FPRTI. The APC was waived by the journal, i.e. funded by MDPI.

Institutional Review Board Statement: Not applicable, no biological sampling was conducted. Rehabilitation and necropsy of deceased turtles was conducted in accordance with the high standards of Florida Fish and Wildlife Conservation Commission (FWC) under rehabilitation permit MTP-16-228.

Informed Consent Statement: Not applicable.

Data Availability Statement: Data is contained within the article or Supplementary Material.

Acknowledgments: We give our warmest thanks to the veterinary and rehabilitation staff and volunteers of the Sea Turtle Hospital at Whitney Laboratories and to Mark Q. Martindale and Nancy Condrón.

Conflicts of Interest: The authors declare no conflict of interest.

References

1. White, E.M.; Clark, S.; Manire, C.A.; Crawford, B.; Wang, S.; Locklin, J.; Ritchie, B.W. Ingested Micronizing Plastic Particle Compositions and Size Distributions within Stranded Post-Hatchling Sea Turtles. *Environ. Sci. Technol.* **2018**, *52*, 10307–10316. [[CrossRef](#)] [[PubMed](#)]
2. Morales-Caselles, C.; Viejo, J.; Martí, E.; González-Fernández, D.; Pragnell-Raasch, H.; González-Gordillo, J.I.; Montero, E.; Arroyo, G.M.; Hanke, G.; Salvo, V.S.; et al. An inshore–offshore sorting system revealed from global classification of ocean litter. *Nat. Sustain.* **2021**, *4*, 484–493. [[CrossRef](#)]
3. Ivar Do Sul, J.A.; Costa, M.F. The present and future of microplastic pollution in the marine environment. *Environ. Pollut.* **2014**, *185*, 352–364. [[CrossRef](#)] [[PubMed](#)]
4. Ryan, P.G. Ingestion of Plastics by Marine Organisms. In *Hazardous Chemicals Associated with Plastics in the Marine Environment*; Takada, H., Karapanagioti, H.K., Eds.; Springer International Publishing: Cham, Switzerland, 2019; pp. 235–266. [[CrossRef](#)]
5. Savoca, M.S.; McInturf, A.G.; Hazen, E.L. Plastic ingestion by marine fish is widespread and increasing. *Glob. Change Biol.* **2021**, *27*, 2188–2199. [[CrossRef](#)] [[PubMed](#)]
6. Alava, J.J. Modeling the Bioaccumulation and Biomagnification Potential of Microplastics in a Cetacean Foodweb of the North-eastern Pacific: A Prospective Tool to Assess the Risk Exposure to Plastic Particles. *Front. Mar. Sci.* **2020**, *7*, 566101. [[CrossRef](#)]
7. Pozo, K.; Gomez, V.; Torres, M.; Vera, L.; Nuñez, D.; Oyarzún, P.; Mendoza, G.; Clarke, B.; Fossi, M.C.; Baini, M.; et al. Presence and characterization of microplastics in fish of commercial importance from the Biobío region in central Chile. *Mar. Pollut. Bull.* **2019**, *140*, 315–319. [[CrossRef](#)]
8. Cox, K.D.; Covernton, G.A.; Davies, H.L.; Dower, J.F.; Juanes, F.; Dudas, S.E. Human Consumption of Microplastics. *Environ. Sci. Technol.* **2019**, *53*, 7068–7074. [[CrossRef](#)]
9. Rummel, C.D.; Jahnke, A.; Gorokhova, E.; Kühnel, D.; Schmitt-Jansen, M. Impacts of biofilm formation on the fate and potential effects of microplastic in the aquatic environment. *Environ. Sci. Technol. Lett.* **2017**, *4*, 258–267. [[CrossRef](#)]
10. Yaranal, N.A.; Subbiah, S.; Mohanty, K. Distribution and characterization of microplastics in beach sediments from Karnataka (India) coastal environments. *Mar. Pollut. Bull.* **2021**, *169*, 112550. [[CrossRef](#)]
11. Lots, F.A.E.; Behrens, P.; Vijver, M.G.; Horton, A.A.; Bosker, T. A large-scale investigation of microplastic contamination: Abundance and characteristics of microplastics in European beach sediment. *Mar. Pollut. Bull.* **2017**, *123*, 219–226. [[CrossRef](#)]
12. Efimova, I.; Bagaeva, M.; Bagaev, A.; Kileso, A.; Chubarenko, I.P. Secondary microplastics generation in the sea swash zone with coarse bottom sediments: Laboratory experiments. *Front. Mar. Sci.* **2018**, *5*, 313. [[CrossRef](#)]
13. Eastman, C.B.; Farrell, J.A.; Whitmore, L.; Rollinson Ramia, D.R.; Thomas, R.S.; Prine, J.; Eastman, S.F.; Osborne, T.Z.; Martindale, M.Q.; Duffy, D.J. Plastic Ingestion in Post-hatchling Sea Turtles: Assessing a Major Threat in Florida Near Shore Waters. *Front. Mar. Sci.* **2020**, *7*, 693. [[CrossRef](#)]
14. Di Renzo, L.; Mascilongo, G.; Berti, M.; Bogdanović, T.; Listeš, E.; Brkljača, M.; Notarstefano, V.; Gioacchini, G.; Giorgini, E.; Olivieri, V.; et al. Potential Impact of Microplastics and Additives on the Health Status of Loggerhead Turtles (*Caretta caretta*) Stranded Along the Central Adriatic Coast. *Water Air Soil Pollut.* **2021**, *232*, 98. [[CrossRef](#)]
15. Rice, N.; Hiram, S.; Witherington, B. High frequency of micro- and meso-plastics ingestion in a sample of neonate sea turtles from a major rookery. *Mar. Pollut. Bull.* **2021**, *167*, 112363. [[CrossRef](#)]
16. Osborne, T.Z.; Ellis, L.R. *Removal of Organic Matter from Hydric Soils for Textural Analysis using Hydrogen Peroxide*; St. Johns River Water Management District: Palatka, FL, USA, 2013.
17. Gal, S.; Premovic, P. Density Determination of Plastics by a Volumetric Titration Method. *Die Angew. Makromol. Chem.* **1980**, *84*, 1–6. [[CrossRef](#)]
18. *BS ISO 3507:1999*; Laboratory Glassware. Pyknometers. ISO: Geneva, Switzerland, 1999.
19. Saliu, F.; Montano, S.; Garavaglia, M.G.; Lasagni, M.; Seveso, D.; Galli, P. Microplastic and charred microplastic in the Faafu Atoll, Maldives. *Mar. Pollut. Bull.* **2018**, *136*, 464–471. [[CrossRef](#)]
20. Höhne, G.; Hemminger, W.F.; Flammersheim, H.-J. *Differential Scanning Calorimetry*; Imprint; Springer: Berlin/Heidelberg, Germany, 2003.
21. Brandrup, J.; Immergut, E.H. (Eds.) *Polymer Handbook*; Interscience Publishers: Geneva, Switzerland, 1966.
22. Silverstein, R.M.; Robert, M.; Bassler, G.C. *Spectrometric Identification of Organic Compounds*; Wiley: Hoboken, NJ, USA, 1967.
23. Mostafa, H.S.; John, H.; Lienhard, V.; Syed, M.Z. Thermophysical properties of seawater: A review of existing correlations and data. *Desalination Water Treat.* **2010**, *16*, 354–380.
24. Tu, C.; Chen, T.; Zhou, Q.; Liu, Y.; Wei, J.; Wanek, J.J.; Luo, Y. Biofilm formation and its influences on the properties of microplastics as affected by exposure time and depth in the seawater. *Sci. Total Environ.* **2020**, *734*, 139237. [[CrossRef](#)]
25. Lin, J.; Yan, D.; Fu, J.; Chen, Y.; Ou, H. Ultraviolet-C and vacuum ultraviolet inducing surface degradation of microplastics. *Water Res.* **2020**, *186*, 116360. [[CrossRef](#)]
26. Longo, C.; Savaris, M.; Zeni, M.; Brandalise, R.N.; Grisa, A.M.C. Degradation study of polypropylene (PP) and Bioriented polypropylene (BOPP) in the environment. *Mater. Res.* **2011**, *14*, 442–448. [[CrossRef](#)]
27. Harrold, Z.; Arienzo, M.M.; Collins, M.; Davidson, J.M.; Bai, X.; Sukumaran, S.; Umek, J. A Peristaltic Pump and Filter-Based Method for Aqueous Microplastic Sampling and Analysis. *ACS EST Water* **2022**, *2*, 268–277. [[CrossRef](#)]

-
28. Araujo, C.F.; Nolasco, M.M.; Ribeiro, A.M.P.; Ribeiro-Claro, P.J.A. Identification of microplastics using Raman spectroscopy: Latest developments and future prospects. *Water Res.* **2018**, *142*, 426–440. [[CrossRef](#)] [[PubMed](#)]
 29. Frère, L.; Paul-Pont, I.; Moreau, J.; Soudant, P.; Lambert, C.; Huvet, A.; Rinnert, E. A semi-automated Raman micro-spectroscopy method for morphological and chemical characterizations of microplastic litter. *Mar. Pollut. Bull.* **2016**, *113*, 461–468.